

Filling of Chitosan Film with Wax/Halloysite Microparticles for Absorption of Hydrocarbon Vapors

Maria Rita Caruso, Giulia D'Agostino, Jaromír Wasserbauer, Pavel Šiler, Giuseppe Cavallaro,* Stefana Milioto, and Giuseppe Lazzara

The effect of the preparation protocol of chitosan (CHI) based films filled with wax microparticles stabilized by halloysite nanotubes (HNTs) in Pickering emulsions (PE) is investigated. The obtained results show that the addition of acetic acid (before or after the preparation of wax/HNT microspheres) affects the properties of the composite films as well as the colloidal stability of PE. The colloidal behavior of CHI/HNT/wax PE by optical microscopy and sedimentation tests are studied. On the other hand, the corresponding composite films (prepared by solvent casting method) are characterized through several techniques, including Scanning Electron Microscopy, UV-vis spectrometer, water permeability, and contact angle measurements. Dynamic Mechanical Analysis allows this to estimate the effect of wax microparticles on the tensile performances of CHI-based films. As a general consideration, the filling of the CHI matrix with wax/HNT improves the physicochemical properties of the films. Finally, the efficacy of the films as adsorbents of n-dodecane vapors is explored. Due to the presence of hydrophobic domains (wax embedded in CHI), the composite films possess higher adsorption efficiencies compared to pristine CHI. Accordingly, it can be stated that the combination of CHI with wax/HNT microparticles is promising to obtain biocompatible composite films useful for remediation purposes.

1. Introduction

The study of the adsorption phenomenon of hydrocarbon vapors on natural materials is the object of recent experimental research for application in environmental remediation. Biopolymers have gained attention as sustainable building blocks of smart materials due to their physicochemical characteristics for their application in different industries, such as pharmaceuticals, textiles, food packaging, cosmetics, agriculture, building materials, and cultural heritage. Natural polymers are typically eco-friendly, non-toxic, biocompatible, and biodegradable. Their properties can be tuned by chemical and physical modifications. Chitosan (CHI) is a polysaccharide obtained from chitin by partial N-deacetylation process at temperatures between 60–80 °C using alkalis of 50% w/w. CHI has a crystalline degree lower than chitin, therefore, it is more soluble in reagents and acidic aqueous solutions. Through the literature, it is evidenced that CHI can be used in various

applications, including cosmetics, biomedicine, food packaging, and environmental applications.^[1–7] Pickering Emulsion (PE) has been an object of scientific interest due to the possibility of dispersing hydrophobic compounds in an aqueous solvent through solid substances that act as stabilizers.^[8–12] Due to the extraordinary colloidal stability and the possibility to control the diameter of the oil droplets from 1 nm to several μm, PE are interesting for many versatile applications. Contrary to conventional emulsions obtained by using surfactants as stabilizing agents, PE are always eco-friendly and sustainable. Recently, halloysite nanotubes ($\text{Al}_2\text{Si}_2\text{O}_5(\text{OH})_4 \cdot n\text{H}_2\text{O}$) (HNTs), were investigated as stabilizers of hydrophobic material in water. HNTs are 1:1 phyllosilicates where a silicon layer with tetrahedral geometry (external negative charge) alternates with an aluminum layer with octahedral geometry (internal positive charge) joined together with hydrogen bonds. Among the various layers, there are water molecules that allow the system to have a spiral tubular shape. HNTs are biocompatible and non-toxic nanomaterials.^[13–16] Besides, HNTs possess numerous physicochemical advantages such as active inorganic material, different surface charges with a tubular morphology, mechanical strength, switchable partial surface and wetting properties useful for many

M. R. Caruso, G. D'Agostino, G. Cavallaro, S. Milioto, G. Lazzara
Department of Physics and Chemistry
"Emilio Segrè"

University of Palermo
viale delle scienze Ed. 17, Palermo 90128, Italy
E-mail: giuseppe.cavallaro@unipa.it

G. D'Agostino
Dipartimento di Scienze dell'Antichità
Università degli Studi di Roma "La Sapienza"
Piazzale Aldo Moro 5, Rome 00185, Italy

J. Wasserbauer, P. Šiler
Faculty of Chemistry
Institute of Materials Science
Brno University of Technology
Purkyňova 118, Brno 61200, Czech Republic

 The ORCID identification number(s) for the author(s) of this article can be found under <https://doi.org/10.1002/adsu.202400026>

© 2024 The Author(s). Advanced Sustainable Systems published by Wiley-VCH GmbH. This is an open access article under the terms of the [Creative Commons Attribution-NonCommercial-NoDerivs License](#), which permits use and distribution in any medium, provided the original work is properly cited, the use is non-commercial and no modifications or adaptations are made.

DOI: 10.1002/adsu.202400026

applications, including food packaging,^[17–19] biomedicine,^[20–22] cultural heritage,^[23,24] catalysis,^[25–29] drug delivery,^[30–36] and environmental applications.^[31,37–42] In our previous works,^[24,43] we used HNTs act as stabilizers of wax droplets in the aqueous medium to prepare PE emulsions useful for cultural heritage applications. HNTs formed a physical barrier at the interface of the hydrophobic phase dispersed in water. The wax inner core generated a hydrophobic layer on the artwork surface helpful in outdoor expositions with weather conditions that can cause alterations and degradation. Moreover, HNTs allowed to disperse the wax in water and improve the thermal and mechanical properties of the coating. PE was designed by microspheres of wax covered with HNTs in hydroxypropyl cellulose^[43] or pectin^[24] matrix as coatings for the conservation of archaeological woods and stone surfaces. In this work, we investigated PE films consisting of wax/HNT microparticles in a CHI matrix as absorbers of hydrocarbon vapors for remediation purposes. In the first part, we studied the preparation protocol of PE in a CHI matrix. Two preparation protocols were carried out to see the effect of acetic acid addition in the formation of wax/HNT microparticles. The emulsions were analyzed under an optical microscope to identify the size of the droplets and subsequently, the colloidal stability was studied. Films were created from PE by solvent casting method, and they were observed by Scanning Electron Microscopy. Transparency, water contact angle, water vapor permeability, and tensile performances were studied to achieve a complete description on the properties of the films. In conclusion, a novel promising biopolymer-based material with active wax microparticles stabilized in water with HNTs has been created for the removal of hydrocarbon vapors.

2. Experimental Section

2.1. Material

Chitosan (CHI, Mw = 50000–190,000 Da, deacetylation degree = 75–85%), microcrystalline wax (melting point from 45 to 58 °C) and Acetic Acid (CH₃COOH) are Sigma–Aldrich products. Halloysite nanotubes (HNTs) are a gift from I-Minerals Inc. Calcium chloride dihydrate (≥99%) is from Panreac, while n-dodecane is from Fluka.

2.2. Methods

2.2.1. Preparation of Pickering Emulsions and Composite Films

Since CHI was soluble in an acid environment, it was decided to proceed with two parallel but different protocols to prepare Pickering emulsion to investigate if the preparation method can affect the chemical and physical characteristics of the films. In the first protocol, Pickering Emulsion was designed as reported in the previous work.^[43] Briefly, water was heated up to 90 °C, and 0.25 wt.% of wax was added under magnetic stirring. After the complete melting of wax, HNTs were added to the wax-in-water system at a concentration of 1.5 wt. % and the dispersion

was subjected to ultrasounds for 10 min and was stirred at high-temperature conditions for 30 min. At this point, the heating system was turned off to cool down the Pickering emulsion while stirring for 24 h. After one day, acid acetic at a concentration of 0.5 wt.% was added under a magnetic stirrer for 30 min. CHI at a concentration of 1 wt.% was added to the Pickering emulsion, and it was left under a magnetic stirrer for one night to dissolve CHI completely within the emulsion (PE/CHI/POST). For the second preparation protocol these were proceeded to add to the acetic acid solution (0.5 wt.%) at a temperature of 90 °C, the wax (0.25 wt.%) until complete melting under magnetic stirring, and then combined HNTs (1.5 wt. %). The dispersion was ultrasonicated for 10 minutes, magnetically stirred for 30 minutes at 90 °C, and afterward, cooled down while stirring at room temperature for 24 h. After one day, CHI at a concentration of 1 wt.% was added to the Pickering emulsion and it was left under a magnetic stirrer for one night to dissolve CHI within the emulsion (PE/CHI/PRE). Two Pickering emulsions were obtained in a CHI matrix. Both emulsions appear creamy white and stable. A CHI solution at 1 wt.% was prepared to compare the system with pure CHI. A solution of acetic acid at 0.5 wt.% was prepared under magnetic agitation, and subsequently, CHI was added at 1 wt.%. The solution was left in a magnetic stirrer for one night to completely dissolve the polymer.

Composite films based on CHI and wax/HNTs microparticles were prepared from the Pickering emulsions by using the solvent casting method as reported elsewhere for pectin^[24] and hydroxypropyl cellulose.^[43] Specifically, PE/CHI/PRE and PE/CHI/POST emulsions were poured into a petri dish (10 cm diameter) and left for 48 h in a vacuum chamber for a complete evaporation of the solvent. The corresponding films were defined as CHI/WAX/PRE and CHI/WAX/POST. For comparison, the film based on pristine CHI was prepared by using the same procedure.

2.2.2. Absorption Tests of Hydrocarbon Vapors

The absorption tests of hydrocarbon vapor were performed in a desiccator saturated with n-dodecane at 25 °C and 65% relative humidity. The percentages of absorbed vapor (Abs%) onto films were determined through the gravimetric method at variable times (1, 6, 11, and 18 days). The ability to absorb vapor from the films was calculated by the following Equation (1)

$$\text{Abs\%} = [(M_t - M_0) / M_0] \cdot 100 \quad (1)$$

where M_0 is the initial mass (before the exposure to the vapors) of the film, while M_t is the mass of the film after a certain exposure time to n-dodecane vapors.

2.2.3. Optical Microscopy

A digital microscope, (Dino-Lite 20X-200X), was used to image WAX/HNT microspheres in a CHI matrix and CHI/WAX/PRE and CHI/WAX/POST emulsions.

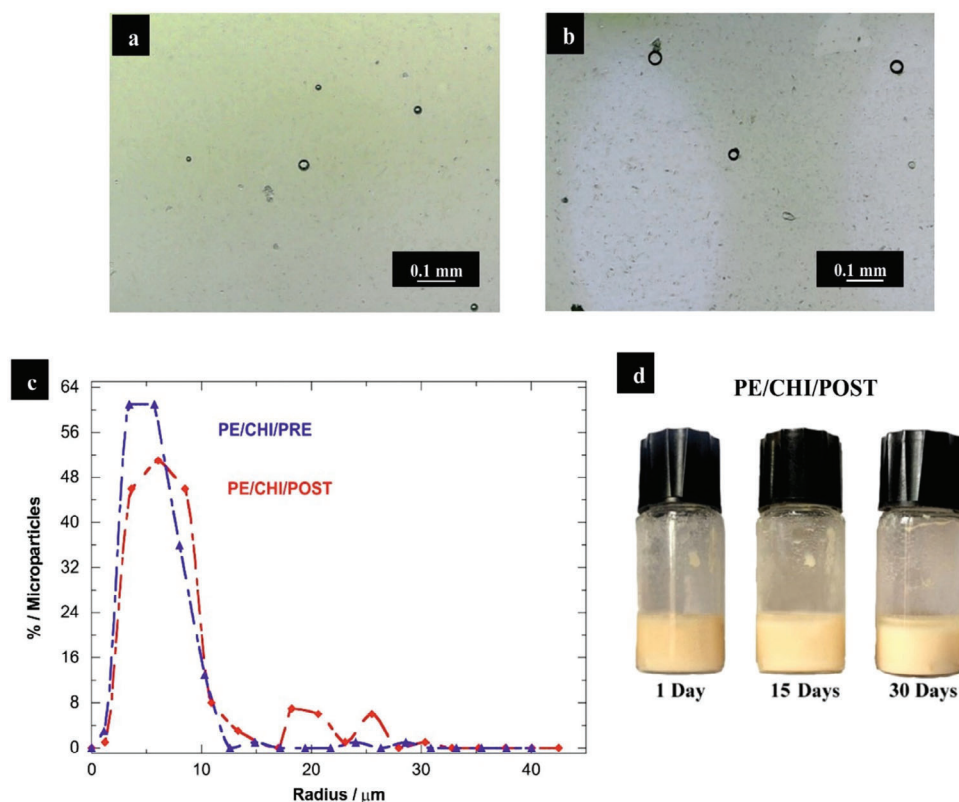


Figure 1. Optical microscopies of PE/CHI/PRE a) and PE/CHI/POST b) and the corresponding sizes distributions of the wax/HNTs droplets c). Images of PE/CHI/POST after variable times from the preparation d).

2.2.4. Film Transparency Analysis

Film transparency was investigated by using a Beckman spectrophotometer (model DU-640). An absorption spectrum was determined as

$$A = 2 - \log (\%T) \quad (2)$$

where T is the transmittance. The attenuation coefficient for each sample was calculated as

$$K = A / (2.3 \cdot D) \quad (3)$$

where A is the absorbance and D is the thickness of the film measured with a micro-meter ($\pm 10^{-2}$ mm).

2.2.5. Scanning Electron Microscopy (SEM)

The surface morphology and microstructure on fracture surfaces were imaged by scanning electron microscope Zeiss EVO LS 10. Secondary electron mode with an acceleration voltage of 15 kV and a working distance of 12 mm was used. All samples were sputtered with gold to avoid surface charging and improve the image quality.

2.2.6. Contact Angle Analysis

The surface behavior of films was examined with contact angle apparatus (OCA 20, Data Physics Instruments) equipped with a video measuring system having a high-resolution CCD camera and a high-performance digitizing adapter. The contact angle (θ) of water in the air was determined by the sessile drop method by gently placing a droplet of $12.0 \pm 0.5 \mu\text{L}$ onto the surface of the rectangular films ($1 \times 2 \text{ cm}^2$), fixed on top of a sample holder with double-sided tape and kept flat throughout the analysis. A minimum of 2 droplets was examined for each film sample. Images were collected 25 times per evolution of θ , starting from the deposition of the drop to 60 s. SCA 20 software (Data Physics Instruments) was used for data acquisition.

2.2.7. Water Permeability Analysis

The tests were carried out in a desiccator at a temperature of $27 \pm 2 \text{ }^\circ\text{C}$ and $30 \pm 2\%$ relative humidity using a saturated solution of calcium chloride dihydrate. Films were cut into a circular shape, the diameters of which were larger than the inner diameter of the bottle (25 mL, 1.5 cm inner diameter), and they were fixed, by using a modeling paste, on the top of each bottle filled with water. Samples were placed in a desiccator and a thermohygrometer was placed inside the equipment to confirm the environmental parameters. The water transferred through the films

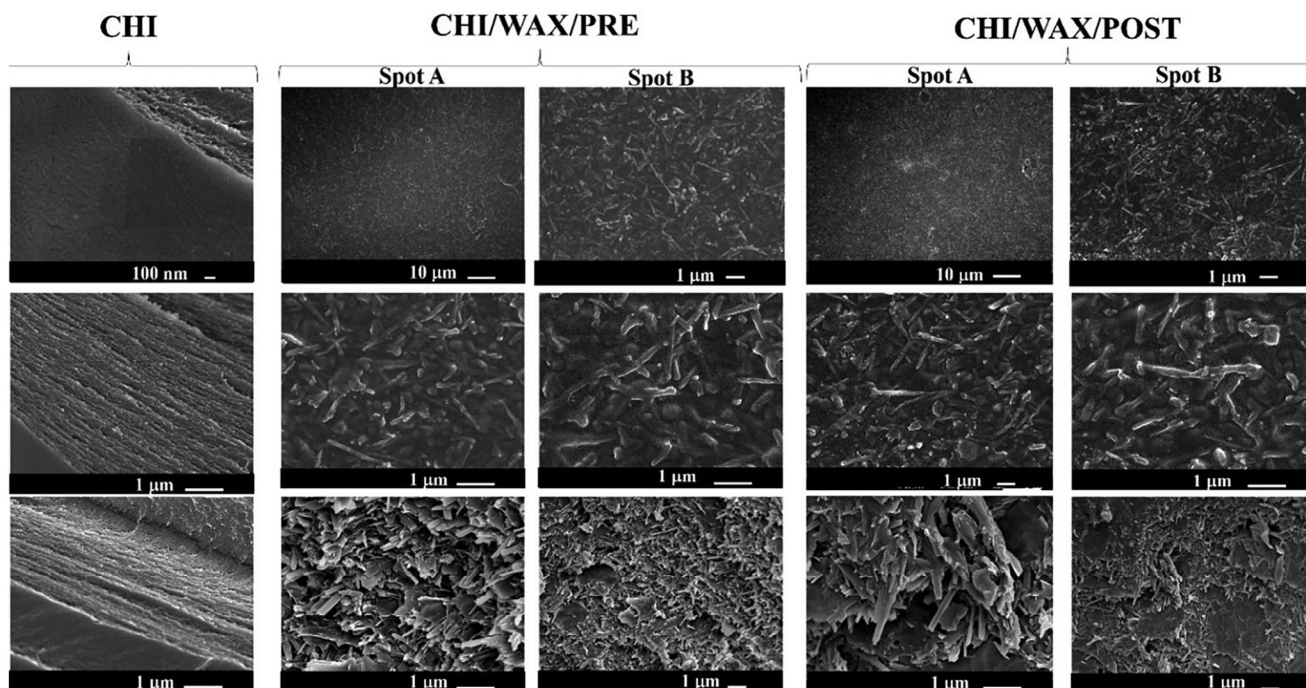


Figure 2. SEM images of films based on pristine CHI and composites (CHI/WAX/PRE and CHI/WAX/POST). SEM images of composite materials refer to different spots (spot A and spot B) of the films.

and absorbed by the desiccant, was determined from the weight loss of the bottle after every hour for a 6 h period using a balance (± 0.00001 g) and then after 24 h, and 2 days.

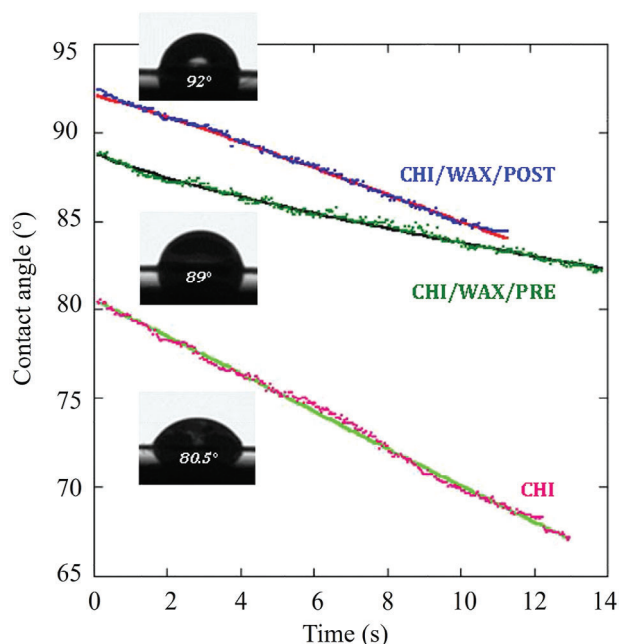


Figure 3. θ versus time curves for pure CHI film and films containing HNT/wax particles. The insets display the water droplet images immediately after their deposition on the film surface with the corresponding contact angle values.

transmission rate (WVTR) and water vapor permeability (WVP) were calculated as

$$\text{WVTR} = (\Delta m / \Delta t \cdot SA) \quad (4)$$

$$\text{WVP} = \text{WVTR} (L / \Delta p) \quad (5)$$

where $\Delta m / \Delta t$ is the slope of each line obtained from the weight loss of samples over time (g/h), SA is the exposed surface area of the film (m^2), L is the thickness of the film (m), and Δp is the difference of partial pressure (Pa) between saturated solution at 32% of relative humidity and saturation water vapor pressure at a temperature of 27 °C.

2.2.8. Dynamic Mechanical Analysis (DMA)

Dynamic Mechanical Analysis (DMA) was conducted by a DMA Q800 apparatus (TA Instruments) to evaluate the tensile properties of films. Rectangular samples of films were studied under a stress ramp of 1 MPa min^{-1} at 25.0 ± 0.5 °C. The analysis of the stress versus strain curves allowed us to determine the tensile performances of the films in terms of Young modulus, ultimate elongation, stress at breaking, and yield points.

3. Results and Discussion

3.1. Morphology and Colloidal Stability of Pickering Emulsions

The preparation protocol of wax/HNTs microspheres in aqueous media is presented in the previous works.^[24,43] We detected

that the presence of acetic acid, which is needed to solubilize CHI, does not prevent the formation of wax microspheres stabilized in water by HNTs. As shown **Figure 1a,b**, this finding is valid for both employed preparation protocols. We conducted a statistical analysis on the sizes of the wax droplets by using ImageJ software allowing us to investigate the influence of the acetic acid addition (PRE or POST) toward the geometrical characteristics of the microparticles. It can be observed that curves are comparable, indeed the graph (**Figure 1c**) shows a most frequent radius value of $\approx 10 \mu\text{m}$ for 61% and 51% of particles for PE/CHI/PRE and PE/CHI/POST, respectively. In general, the density number of wax droplets dispersed in the aqueous medium is higher for PE/CHI/POST. Furthermore, it should be noted that PE/CHI/POST emulsion presents larger particles (average radii of 20 and 28 μm), which were not detected in the PE/CHI/PRE system. Moreover, the addition of CHI influenced the colloidal stability of wax/HNTs Pickering emulsions. The colloidal behavior of the emulsions was macroscopically monitored for variable times. As shown in **Figure 1d**, PE/CHI/POST is stable even after 30 days from the preparation. Similar observations were obtained for PE/CHI/PRE, while PE without CHI exhibited complete separation after 8 days.^[43] These results highlighted that the CHI addition improves the colloidal stability of wax/HNTs microspheres in water that might be related to their sizes, which are reduced by the presence of the biopolymer in agreement with our previous studies^[24,43] concerning the effects of pectin and hydroxypropyl cellulose on wax/HNT Pickering emulsions.

3.2. Surface Properties and Transparency of the Films

Figure 2 shows the SEM images of CHI, CHI/WAX/PRE, and CHI/WAX/POST samples. As concerns the composite materials, we collected SEM micrographs from two different spots (spot A and spot B) to evaluate the homogeneity of the microstructural characteristics of the films.

The film based on pristine CHI evidenced a smooth surface, while the cross section showed a flake-like structure. Differently, the composites with wax and HNTs evidenced a rough surface with clay nanotubes embedded into the polymeric matrix. The HNTs dispersion is homogeneous on the film surface of both CHI/WAX/PRE and CHI/WAX/POST as evidenced by the similar morphologies detected from spots A and B. Based on SEM images, we can assert that clay nanotubes do not form aggregates on the film surface. Moreover, we observed that the nanotubes are randomly distributed, and they do not present any orientation. It should be noted that the flake-like structure of the transversal section is not observed in both composites. Clearly, the wax location cannot be assessed directly by SEM images due to the lack of contrast between CHI and wax.

The surface properties (chemical composition and roughness) of the films influence their wettability characteristics, which are related to their water affinity. Water contact angle (θ) analysis allows us to investigate water absorption/spreading phenomena at the film surface.

As shown in **Figure 3**, θ versus time curves exhibited exponential decay functions for pristine CHI and both composite films.

Table 1. Fitting parameters obtained by analysis of water contact angle data.

Film	θ_i [°]	k_θ [s ⁻ⁿ]	n
CHI	80.5	0.0120 ± 0.0001	1.00 ± 0.05
CHI/WAX/PRE	89	0.0099 ± 0.0001	0.78 ± 0.06
CHI/WAX/POST	92	0.0060 ± 0.0001	1.00 ± 0.06

The quantitative analysis of the θ versus time functions was carried out by means of the following Equation (6)

$$\theta = \theta_i \exp(-k_\theta \tau^n) \quad (6)$$

where (θ_i) is the zero-time extrapolated contact angle, k_θ measures the process rate, and n assumes fractional values ascribable to the occurrence of absorption and spreading process. The equation successfully fitted our data providing the parameters reported in **Table 1**. The n values are n = 0 and 1 for pure absorption and pure spreading, respectively. We detected that pure spreading occurs for pristine CHI and CHI/WAX/POST films, while the coexistence of spreading and absorption phenomena was estimated for CHI/WAX/PRE film being that n is 0.78. The latter (n > 0.5) indicates that the spreading is the predominant process. The k_θ values highlighted that the kinetic evolution of the water contact angle is slower for both films with wax/HNTs microparticles compared to pristine CHI film.

Despite the preparation method, wax/HNTs addition caused an increase of θ_i in agreement with the more hydrophobic nature of the surface compared to pure CHI film. The preparation protocol slightly affected the surface hydrophobization of the CHI-based film. Specifically, CHI/WAX/POST film ($\theta_i = 92^\circ$) is slightly more hydrophobic with respect to CHI/WAX/PRE ($\theta_i = 89^\circ$). These results could be related to the effect of acetic acid on the formation of wax droplets. The addition of acetic acid during the preparation of Pickering emulsions (PE/CHI/PRE) reduced the formation of wax microparticles and consequently, the surface hydrophobization on the CHI film is lower compared to CHI/WAX/POST. As a general consideration, the enhanced hydrophobicity of the composite films can be related to variations of the surface chemical composition (due to the presence of wax) and an increase in the roughness.

We studied the optical characteristics of CHI-based films by spectrophotometric measurements. In particular, we estimated the effects of wax/HNTs microparticles on the transparency of the films. This property is crucial to evaluate the suitability of coating film materials for technological applications within several fields. **Figure 4** reports the dependences of the linear attenuation coefficient (K) on the wavelength in vis region for CHI, CHI/WAX/PRE, and CHI/WAX/POST. As a general result, the presence of wax/HNTs microparticles increased the K values of CHI film. The preparation protocol influenced the transparency of the composite films. We observed that CHI/WAX/POST is less transparent compared to CHI/WAX/PRE. This finding agrees with the sizes distributions of Pickering emulsions (**Figure 1**), which evidenced that PE/CHI/POST presents microparticles with larger sizes (20–28 μm) that were not detected in PE/CHI/PRE.

3.3. Water Permeability and Tensile Performances of CHI-based Films

The water transport properties through the prepared films were investigated by measuring the water vapor permeability. Wax/HNTs microparticles on a biopolymer matrix can impact on the vapor permeability parameters. CHI film has a smaller WVP value ($(2.53 \pm 0.33) \cdot 10^{-4} \text{ g} \cdot \text{mm h}^{-1} \text{ m}^2 \text{ Pa}$) compared to the films filled with wax/HNTs microparticles. Specifically, we calculated WVP values of $(4.26 \pm 0.34) \cdot 10^{-4}$ and $(4.15 \pm 1.1) \cdot 10^{-4} \text{ g} \cdot \text{mm h}^{-1} \text{ m}^2 \text{ Pa}$ for CHI/WAX/PRE and CHI/WAX/POST, respectively. These results could be correlated to SEM images of the films (Figure 2), which showed that the cross sections of both composite films do not present the flake structure typical of pure CHI. The tensile performances of the films were determined by DMA experiments, which provided the stress versus strain curves presented in Figure 5. The obtained tensile parameters are collected in Table 2.

The presence of wax/HNTs significantly enhanced the Young modulus of CHI film. We calculated increases of 209 and 350% for CHI/WAX/PRE and CHI/WAX/POST, respectively. These results indicate that the composite films are more rigid compared to the pristine biopolymer. Accordingly, we estimated that the ultimate elongation of composites is lower (≈ 1 order) than pure CHI, while the stress at the yield point is enhanced by ≈ 10 MPa. Regarding the stress at breaking point, we detected that the addi-

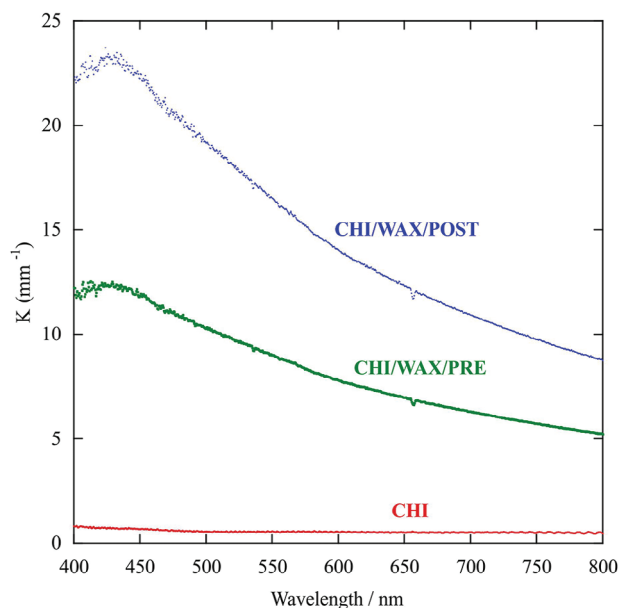


Figure 4. Dependence of the attenuation coefficient (K) on the wavelength (within vis region) for CHI, CHI/WAX/PRE, and CHI/WAX/POST films.

Table 2. Tensile properties of CHI-based films.

Film	Young Modulus (MPa)	Stress at yield point (MPa)	Stress at breaking point (MPa)	Ultimate elongation (%)
CHI	1767 ± 120	34 ± 3	64 ± 4	39.8 ± 1.1
CHI/WAX/PRE	5474 ± 420	43 ± 3	49 ± 3	1.11 ± 0.12
CHI/WAX/POST	8229 ± 720	44 ± 3	54 ± 4	2.08 ± 0.18

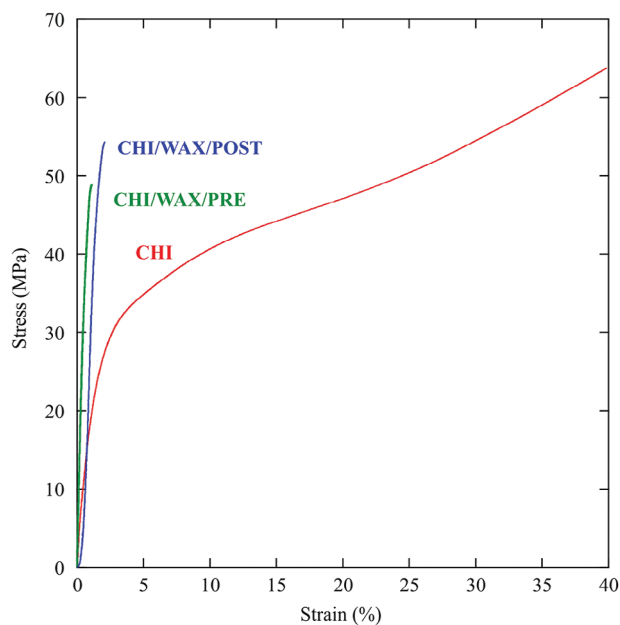


Figure 5. Stress versus strain curves for CHI, CHI/WAX/PRE, and CHI/WAX/POST films.

tion of wax/HNTs generated a decrease indicating that the composite films possess a reduced mechanical resistance. We calculated that CHI/WAX/POST is slightly more resistant with respect to CHI/WAX/PRE film.

3.4. Application of Film as Absorbers of Hydrocarbon Vapor for the Environment

In the previous paragraphs, we demonstrated that the filling of a polymeric matrix with wax/HNTs microparticles by using two different protocols based on Pickering emulsions is effective in controlling the physicochemical properties of CHI films, including their wettability, water permeability, tensile performances, and transparency. Due to the hydrophobicity of microwax particles, the filling processes might be also a perspective to obtain functional films with high absorption capacity toward organic contaminants. Namely, the presence of hydrophobic domains within the CHI matrix can be explored to fabricate coating materials suitable for the removal of pollutants, such as aliphatic and aromatic hydrocarbons. According to this consideration, we tested the absorption efficiency of CHI and composite films toward n-dodecane vapors by gravimetric method. Figure 6 shows the percentage of n-dodecane absorbed on the films at variable exposure times.

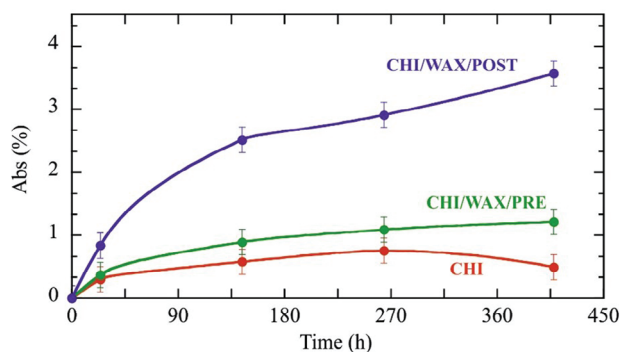


Figure 6. Percentage of n-dodecane absorbed on the films (CHI, CHI/WAX/PRE, and CHI/WAX/POST) as a function of the exposure time toward the hydrocarbon vapors.

As expected, the amount of absorbed n-dodecane is enhanced in the composite films compared to pure CHI. As a general result, the highest absorption efficiency was estimated for CHI/WAX/POST in agreement with its largest surface hydrophobicity (Figure 3). In this regard, it should be noted that CHI/WAX/POST is prepared by the Pickering emulsion (PE/CHI/POST) containing a larger number density of wax droplets with respect to PE/CHI/PRE. Therefore, CHI/WAX/POST presents a greater number of non-polar domains that drive to the n-dodecane absorption because of hydrophobic interactions. The increase of the removal efficiency toward the aliphatic hydrocarbon was detected already after 24 h of exposure time. Specifically, we calculated an increase of $\approx 180\%$ for CHI/WAX/POST with respect to that of pristine CHI. As concerns pristine CHI, we observed that the n-dodecane absorption reaches the saturation at $\approx 0.75\%$ after 11 days, while the removal capacity toward the hydrocarbon vapor was extended over time for both composite films. After 18 days of exposure to n-dodecane vapors, we calculated absorption efficiencies equal to $\approx 1.21\%$ and 3.57% for CHI/WAX/PRE and CHI/WAX/POST, respectively. The obtained data revealed that the removal capacity of CHI-based films can be improved by filling the polymeric matrix with wax/HNTs using the corresponding Pickering emulsions. The preparation protocol plays a crucial role in controlling the absorption capacity of the films. The addition of acetic acid after the preparation of Pickering emulsions is advantageous to enhance the hydrophobic character of the composite film improving its affinity toward n-dodecane vapors. On this basis, CHI-WAX/POST represents a promising absorber material that can be further exploited in the removal strategy of hydrophobic contaminants from vapor and liquid phases.

4. Conclusion

We demonstrated that biopolymeric films with high absorption capacity toward n-dodecane vapors can be obtained by the solvent casting of wax/halloysite Pickering emulsions mixed with chitosan. We detected that the addition of acetic acid (before or after the preparation of Pickering emulsions) affects the properties of the films as well as their absorption efficiency. The addition of acetic acid subsequent to the preparation of Pickering emulsion is advantageous to obtain microwax droplets.

Consequently, the corresponding film (CHI/WAX/POST) exhibited a stronger surface hydrophobization with respect to the film (CHI/WAX/PRE) prepared by adding acetic acid before the preparation of wax/halloysite Pickering emulsions. On the other hand, the preparation protocol did not influence the morphology of the composite films, which presented a uniform distribution of halloysite nanotubes within the chitosan matrix. We observed that the filling of chitosan with wax/HNT microparticles is effective in improving the tensile properties in terms of elastic modulus and stress at the yield point highlighting that the composite films are more rigid. The presence of wax/HNTs within the biopolymeric matrix significantly enhanced the chitosan absorption efficiency toward n-dodecane vapors. After 18 days of exposure to the vapors, we estimated improvements by $\approx 61\%$ and $\approx 195\%$ for CHI/WAX/PRE and CHI/WAX/POST, respectively. These results agree with the larger number density of microwax, which interacts with n-dodecane by hydrophobic attractions, in the CHI/WAX/POST film. In conclusion, this work shows that wax/halloysite Pickering emulsions can be exploited for the preparation of biopolymeric films filled with hydrophobic domains suitable for the solubilization of organic contaminants.

Acknowledgements

The work was financially supported by the PON "Research and Innovation" 2014–2020, Asse IV "Istruzione e ricerca per il recupero", all'Azione IV.5 "Dottorati su tematiche green". DM 1061/2021 and by the University of Palermo.

Conflict of Interest

The authors declare no conflict of interest.

Data Availability Statement

The data that support the findings of this study are available from the corresponding author upon reasonable request.

Keywords

Chitosan, halloysite nanotubes, hydrocarbon vapors absorption, microwax, nanocomposite film

Received: January 9, 2024
Revised: February 9, 2024
Published online: February 24, 2024

- [1] M. R. Caruso, G. D'Agostino, S. Milioto, G. Cavallaro, G. Lazzara, *J. Mater. Sci.* **2023**, *58*, 12954.
- [2] S. Li, H. Wang, D. Huang, J. Liu, C. Chen, D. Li, M. Zhu, Y. Chen, *Adv. Sustain. Syst.* **2022**, *6*, 2200033.
- [3] Y. Jin, Y. He, H. Wang, S. Li, J. Liu, *Adv. Sustain. Syst.* **2023**, *7*, 2300056.
- [4] R. R. Gadkari, S. W. Ali, A. Das, R. Alagirusamy, *Adv. Sustain. Syst.* **2022**, *6*, 2100360.
- [5] E. Santiago, G. Pina-Luis, M. Martinez-Quiroz, O. Perez-Landeros, N. Rosas-González, B. Valdez-Salas, M. T. Oropeza-Guzman, *Adv. Sustain. Syst.* **2021**, *5*, 2000236.

- [6] L. Lisuzzo, G. Cavallaro, G. Lazzara, S. Milioto, *Carbohydr. Polym. Technol. Appl.* **2023**, 6, 100380.
- [7] M. alleshagh, S. Sadjadi, H. Arabi, N. Bahri-Laleh, E. Monflier, *Mater. Chem. Phys.* **2022**, 278, 125506.
- [8] P. G. Sieben, F. Wypych, R. A. de Freitas, *Appl. Clay Sci.* **2022**, 216, 106378.
- [9] A. Panchal, L. T. Swientoniewski, M. Omarova, T. Yu, D. Zhang, D. A. Blake, V. John, Y. M. Lvov, *Colloids Surf. B Biointerfaces* **2018**, 164, 27.
- [10] C. S. Sia, H. P. Lim, Y. N. Lin, L. C. Beh, B. T. Tey, B.-H. Goh, L. E. Low, *Eur. Polym. J.* **2023**, 186, 111870.
- [11] C. Cionti, G. Vavassori, E. Pargoletti, D. Meroni, G. Cappelletti, *J. Colloid Interface Sci.* **2022**, 628, 82.
- [12] L. Liu, X. Pu, H. Tao, K. Chen, W. Guo, D. Luo, Z. Ren, *Colloids Surf. Physicochem. Eng. Asp.* **2021**, 610, 125694.
- [13] X. Wang, J. Gong, R. Rong, Z. Gui, T. Hu, X. Xu, *J. Agric. Food Chem.* **2018**, 66, 2925.
- [14] W. Xue, G. Jiachun, G. Zongxiang, H. Tingting, X. Xiaolong, *Environ. Toxicol.* **2018**, 33, 623.
- [15] E. Tarasova, E. Naumenko, E. Rozhina, F. Akhatova, R. Fakhrullin, *Appl. Clay Sci.* **2019**, 169, 21.
- [16] E. Rozhina, S. Batasheva, R. Miftakhova, X. Yan, A. Vikulina, D. Volodkin, R. Fakhrullin, *Appl. Clay Sci.* **2021**, 205, 106041.
- [17] G. Gorrasi, *Carbohydr. Polym.* **2015**, 127, 47.
- [18] E. Boccalon, P. Sassi, L. Pioppi, A. Ricci, M. Marinozzi, G. Gorrasi, M. Nocchetti, *Appl. Clay Sci.* **2022**, 227, 106592.
- [19] G. Gorrasi, V. Senatore, G. Vigliotta, S. Belviso, R. Pucciariello, *Eur. Polym. J.* **2014**, 61, 145.
- [20] Y. Feng, Y. He, X. Lin, M. Xie, M. Liu, Y. Lvov, *Adv. Healthcare Mater.* **2023**, 12, 2202265.
- [21] Y. Feng, X. Luo, F. Wu, H. Liu, E. Liang, R.-R. He, M. Liu, *Chem. Eng. J.* **2022**, 428, 132049.
- [22] R. Li, Y. Zhang, Z. Lin, Q. Lei, Y. Liu, X. Li, M. Liu, G. Wu, S. Luo, H. Wang, X. Zheng, L. Li, N. Ao, Z. Zha, *Compos. Part B Eng.* **2021**, 221, 109031.
- [23] M. R. Caruso, G. Cavallaro, S. Milioto, G. Lazzara, *Appl. Clay Sci.* **2023**, 238, 106930.
- [24] M. R. Caruso, G. Cavallaro, G. Lazzara, S. Milioto, *Mater. Lett.* **2023**, 133567, 333,.
- [25] S. Sadjadi, N. Abedian-Dehaghani, M. M. Heravi, X. Zhong, P. Yuan, J. Duran, A. Poater, N. Bahri-Laleh, *J. Mol. Liq.* **2023**, 382, 121847.
- [26] S. Sadjadi, G. Lazzara, M. M. Heravi, G. Cavallaro, *Appl. Clay Sci.* **2019**, 182, 105299.
- [27] Y. Liu, H. Guan, J. Zhang, Y. Zhao, J.-H. Yang, B. Zhang, *Int. J. Hydrog. Energy* **2018**, 43, 2754.
- [28] Y. Liu, J. Zhang, H. Guan, Y. Zhao, J.-H. Yang, B. Zhang, *Appl. Surf. Sci.* **2018**, 427, 106.
- [29] A. Glotov, A. Vutolkina, A. Pimerzin, V. Vinokurov, Y. Lvov, *Chem. Soc. Rev.* **2021**, 50, 9240.
- [30] I. A. Iakovlev, A. Y. Deviatov, Y. Lvov, G. Fakhrullina, R. F. Fakhrullin, V. V. Mazurenko, *ACS Nano* **2022**, 16, 5867.
- [31] Y. Lvov, W. Wang, L. Zhang, R. Fakhrullin, *Adv. Mater.* **2016**, 28, 1227.
- [32] F. Liu, L. Bai, H. Zhang, H. Song, L. Hu, Y. Wu, X. Ba, *ACS Appl. Mater. Interfaces* **2017**, 9, 31626.
- [33] M. Fizir, P. Dramou, N. S. Dahiru, W. Ruya, T. Huang, H. He, *Micromol. Acta.* **2018**, 185, 389.
- [34] A. M. Yamina, M. Fizir, A. Itatahine, H. He, P. Dramou, *Colloids Surf. B Biointerfaces* **2018**, 170, 322.
- [35] L. Lisuzzo, G. Cavallaro, S. Milioto, G. Lazzara, *Appl. Clay Sci.* **2024**, 247, 107217.
- [36] G. Cavallaro, G. Lazzara, S. Milioto, *Int. J. Biol. Macromol.* **2023**, 234, 123645.
- [37] O. Owoseni, Y. Su, S. Raghavan, A. Bose, V. T. John, *J. Colloid Interface Sci.* **2022**, 620, 135.
- [38] O. Owoseni, E. Nyankson, Y. Zhang, S. J. Adams, J. He, G. L. McPherson, A. Bose, R. B. Gupta, V. T. John, *Langmuir* **2014**, 30, 13533.
- [39] P. Maziarz, J. Matusik, A. Radziszewska, *J. Environ. Chem. Eng.* **2019**, 7, 103507.
- [40] Y. Chen, S. Krings, A. M. J. M. Beale, B. Guo, S. Hingley-Wilson, J. L. Keddie, *Adv. Sustain. Syst.* **2022**, 6, 2200312.
- [41] H. Mansouri, H. Ait Said, H. Noukrati, A. Oukarroum, H. Ben youcef, F. Perreault, *Adv. Sustain. Syst.* **2023**, 7, 2300149.
- [42] N. V. Patil, A. N. Netravali, *Adv. Sustain. Syst.* **2019**, 3, 1900009.
- [43] L. Lisuzzo, M. R. Caruso, G. Cavallaro, S. Milioto, G. Lazzara, *Ind. Eng. Chem. Res.* **2021**, 60, 1656.